

Boost Converter with nonisolated Multiinput Multioutput for Energy Management in Hybrid Electric Vehicles

MEENU MANIKUTTAN¹, JEEMA K CHERIAN²

¹MTech student, ²Associate Professor
Department of Electrical and Electronics
NSS College of Engineering, Palakkad

Abstract— A new multiinput multioutput dc–dc boost converter with unified structure for hybridizing of power sources in electric vehicles is proposed. The proposed converter can be used for transferring energy between different energy resources. The converter has two main operation modes which in battery discharging mode all input sources deliver power to output and in battery charging mode main energy system not only supplies loads but also delivers power to the rechargeable energy storage systems. It is possible to have several outputs with different dc voltage levels are appropriate for connection to multilevel inverters. In electric vehicles, using of multilevel inverters leads to torque ripple reduction of induction motors. Also, electric vehicles which use dc motors have at least two different dc voltage levels, one for ventilation system and cabin lighting and other for supplying electric motor.

Index Terms— Boost converter, fuel cell, hybrid electric vehicle, multiple input multiple output, nonisolation, small signal modeling, rechargeable energy storage systems.

1 INTRODUCTION

THE large number of automobiles in use around the world has caused and continues to cause serious problems of environment and human life. Air pollution, global warming, and the rapid depletion of the earth's petroleum resources are now serious problems. Electric Vehicles (EVs), Hybrid Electric Vehicles (HEVs) and Fuel Cell Electric Vehicles (FCEVs) have been typically proposed to replace conventional vehicles in the near future. Most electric and hybrid electric configurations use two energy storage devices, one with high energy storage capability, called the "main energy system" (MES), and the other with high power capability and reversibility, called the "rechargeable energy storage system" (RESS). MES provides extended driving range, and RESS provides good acceleration.

Fuel cells (FCs) are emerging as a promising main power sources due to their merits of cleanness, high efficiency, and high reliability. Because of long startup period and slow dynamic response weak points of FCs [1], mismatch power between the load and the FC must be managed by an energy storage system. Batteries are usually taken as storage mechanisms for smoothing output power, improving startup transitions and dynamic characteristics, and enhancing the peak power capacity. Combining such energy sources introduces a FC/battery hybrid power system. In comparison with single-sourced systems, the hybrid power systems have the potential to provide high quality, more reliable, and efficient power. FC and RESSs have different voltage levels. So, to provide a specific

voltage level for load and control flow between input sources, using of a dc–dc converter for each of the input sources is need. Which leads to increase of price, mass, and losses. Consequently, in hybrid power systems, multiinput dc–dc converters have been used. In isolated multiinput dc–dc converters, high-frequency transformer is used in order to make electric isolation [2]. Using isolation transformer in isolated dc–dc converters will make the system heavy and massive. These converters require inverters in input sides of transformer for conversion of input dc voltage to ac and also need rectifiers in outputs of transformer for conversion of ac voltage to dc. Therefore, in all input and output terminals of these converters, several switches are applied which leads to increase of cost and losses. Furthermore, transformer has losses in its core and windings. Because of the aforementioned drawbacks of isolated multiinput dc–dc converters, usage of nonisolated multiinput dc–dc converters in electric vehicle applications seems more useful [3]–[5]. Comparing to the isolated one, nonisolated multiinput features compact design and high-power density [6].

In [7]–[9], introduced converter consists of paralleling two buck converter in their inputs. To prevent short circuit of sources one switch is series to each input source. Advantage of this converter is less number of energy storage elements and drawback is lack of proper power flow control between input sources. In [10], the converter has four input by different voltages. Each of the energy sources can deliver or absorb energy from load and other sources. Each input source need separate inductor is a shortcoming of the converter. In [11] converter structure derived from cascading two H-bridge with different dc-link voltages. The merit of this converter is its less number of passive elements, and its drawback is unsuitable

- Menu Manikuttan is with Electrical and Electronics Department, NSS College of Engineering, Palakkad (e-mail meenumanikuttan@gmail.com)
- Jeema K Cheria is with Electrical and Electronics Department, NSS College of Engineering, Palakkad (e-mail jeemarajan4@gmail.com)

control on the power which is drawn from input sources. In [12], the converter used a coupled inductor, instead of two separate inductors as energy storage element. The converter is for power management between battery, SC, and electric motor in an electric vehicle. The advantage of this converter is regeneration of brake energy to battery and SC is possible. In electric vehicles, using of multilevel inverters leads to torque ripple reduction of induction motors. For appropriate connection to multilevel inverters outputs with different dc voltage levels needed. One way to generate several dc-links is usage of multioutput dc-dc converters [13]. In [14] and [15], nonisolated multiinput multioutput converter has large number of switches which cause low efficiency.

A new nonisolated multiinput multioutput dc-dc boost converter is proposed in this paper. This converter is applicable in hybridizing alternative energy sources in electric vehicles. In fact, by hybridization of energy sources, advantages of different sources are achievable. Charging or discharging of energy storages by other input sources can be controlled properly. The proposed converter has several outputs with different voltage levels which makes it suitable for interfacing to multilevel inverters.

The organization of this paper is as follows. The converter structure and operation modes are explained in Section 2. Dynamic modelling of the proposed converter is given in Section 3. Section 4 describes the control system of the proposed converter. The simulation results describes in Sections 5. Finally, Section 6 presents the conclusions.

2 CONVERTER STRUCTURE AND OPERATION MODES

A new multiinput multioutput dc-dc boost converter with unified structure for hybridizing of power sources in electric vehicles is proposed which is shown in Fig.1. The proposed converter is suitable alternative for hybridizing of FC, battery, or SC. The converter is appropriate for a connection to a multilevel inverter due to availability of multiinput. Here for convenience, proposed converter with two-input two-output is analyzed. Which is shown in Fig. 2. R_1 and R_2 are the model of load resistances that can represent the equivalent power feeding a multilevel inverter. From the figure 2 understood that source V_{in1} can deliver power to source V_{in2} but not vice versa, so V_{in1} is taken as FC and V_{in2} as battery. Power flow between input sources can be control by proper switching. There are two operation modes for proposed converter depending on the state of battery. In each mode, out of the four switches three are active. Each switch has specific duties.

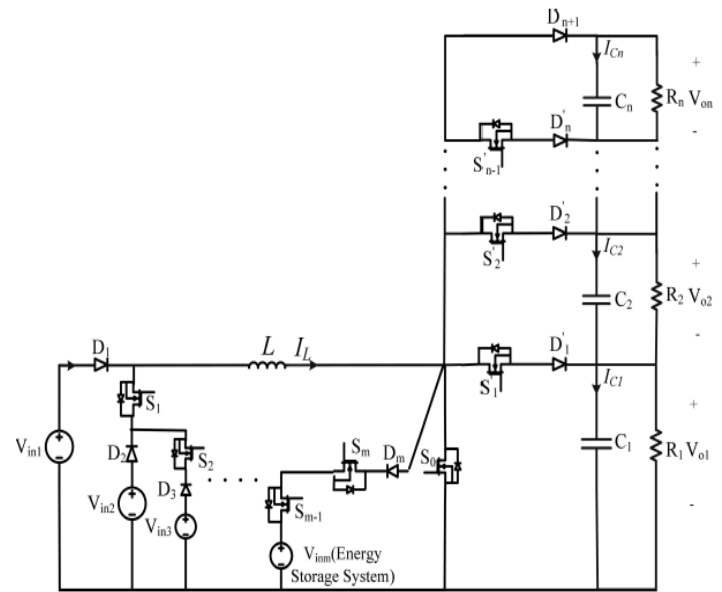


Fig.1 Proposed multiinput multioutput converter.

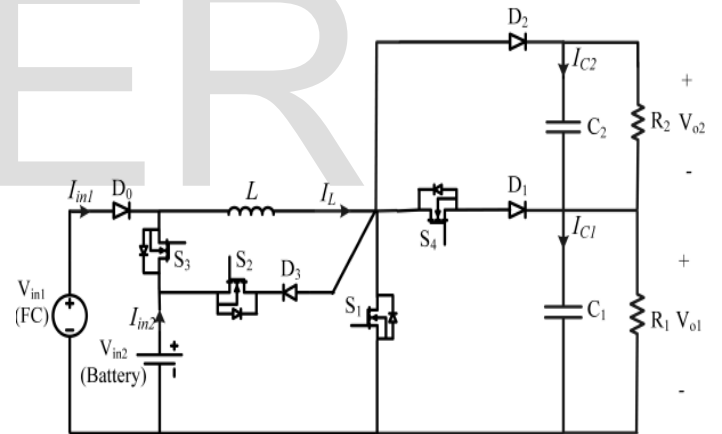


Fig.2 Proposed nonisolated boost converter with two-input, two-output.

2.1 Battery discharging mode

In this mode, both inputs supply power to the loads. Here switch S_1 is on to control battery current to desired value by controlling inductor current. Switch S_3 regulate the total output voltage $V_T = V_{o1} + V_{o2}$ and output voltage V_{o1} is regulate by switch S_4 . In Fig. 3 inductor voltage, Inductor current and gate signal of the switch waveforms are presented. In one switching period there are four different operation modes.

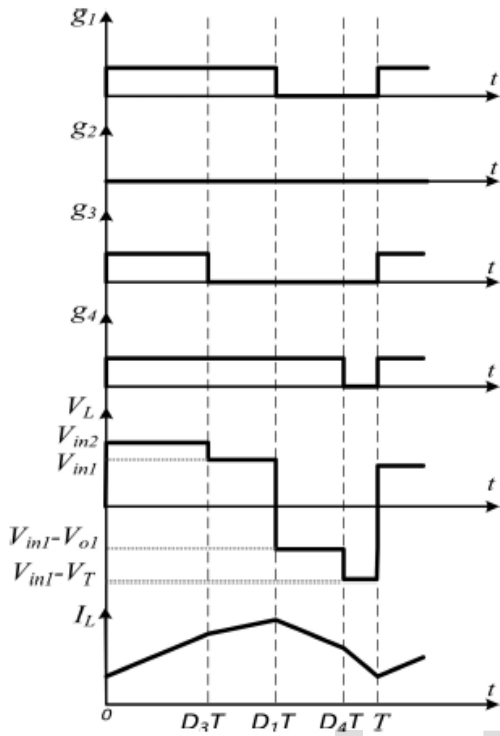


Fig. 3. Steady-state waveforms of proposed converter in battery discharging mode

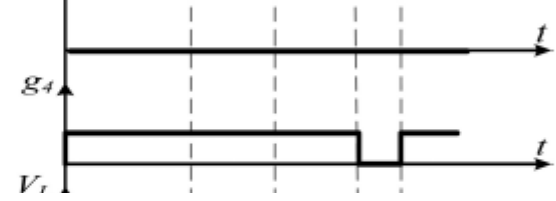


Fig. 5. Steady-state waveforms of proposed converter in battery charging mode

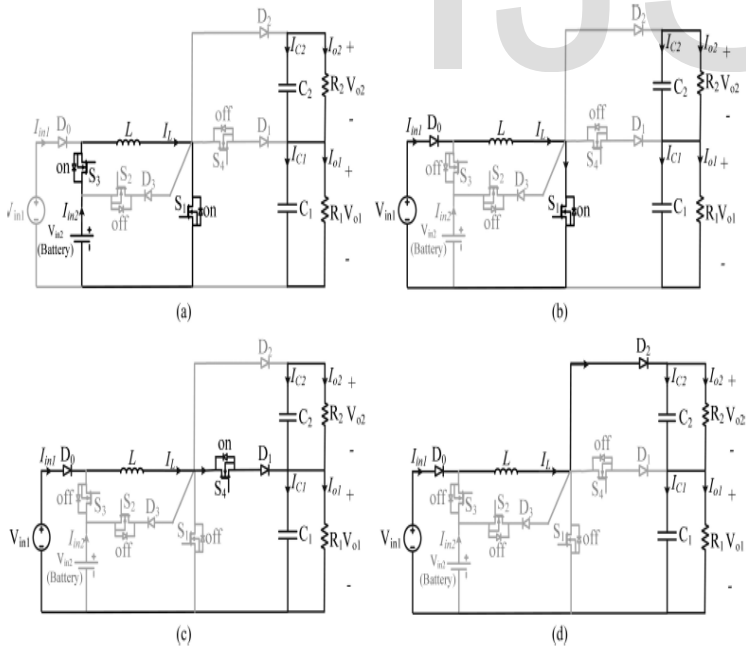


Fig. 4. Equivalent circuit of battery discharging mode, (a) switching state 1, (b) switching state 2, (c) switching state 3, (d) switching state 4.

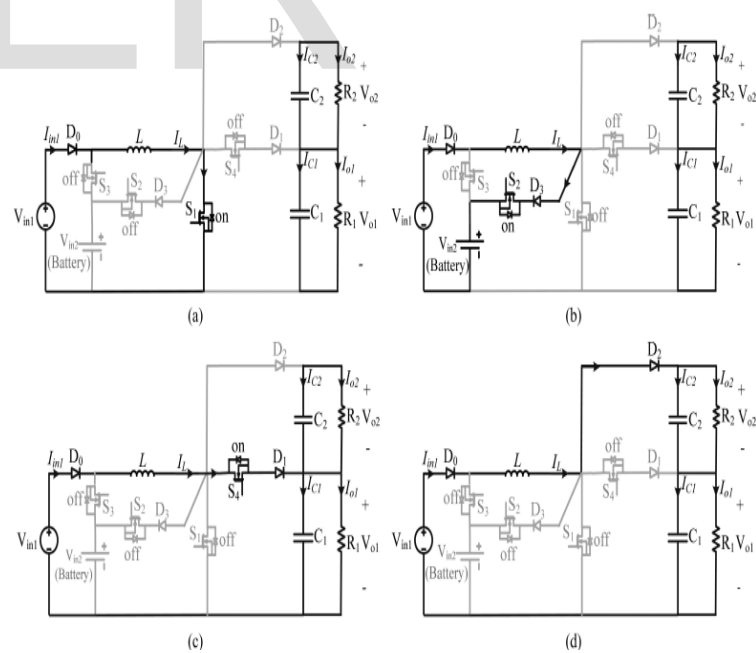


Fig. 6. Battery charging mode, (a) switching state 1, (b) switching state 2, (c) switching state 3, (d) switching state 4.

1) *Switching State* ($0 < t < D_3T$): In this state, switches S_1 and

S_3 are turned ON. Because S_1 is ON, diodes D_1 and D_2 are reversely biased, so switch S_4 is turned OFF. Since S_3 is ON and $V_{in1} < V_{in2}$, diode D_0 is reversely biased. Equivalent circuit of proposed converter in this state is shown in Fig. 4.a. In this state, V_{in2} charges inductor L , so inductor current increases. Also, in this mode, capacitors C_1 and C_2 are discharged and deliver their stored energy to load resistances R_1 and R_2 , respectively. The inductor and capacitors equations in this mode are as follows:

$$\begin{cases} L \frac{dI_L}{dt} = V_{in2} \\ C_1 \frac{dV_{O1}}{dt} = -\frac{V_{O1}}{R_1} \\ C_2 \frac{dV_{O2}}{dt} = -\frac{V_{O2}}{R_2} \end{cases} \quad (1)$$

2) *Switching State 2* ($D_3 T < t < D_1 T$): In this state, switch S_1 is still ON and S_4 is still OFF and S_3 is turned OFF. Because S_1 is ON. Equivalent circuit is shown in Fig. 4(b). In this state V_{in1} charges inductor L , so inductor current increases. In addition, capacitors C_1 and C_2 are discharged and deliver their stored energy to load resistances R_1 and R_2 , respectively. Equations in this mode are as follows:

$$\begin{cases} L \frac{dI_L}{dt} = V_{in1} \\ C_1 \frac{dV_{O1}}{dt} = -\frac{V_{O1}}{R_1} \\ C_2 \frac{dV_{O2}}{dt} = -\frac{V_{O2}}{R_2} \end{cases} \quad (2)$$

3) *Switching State 3* ($D_1 < t < D_4 T$): In this mode, switch S_1 is turned OFF S_4 is turned ON. Fig. 4(c). Inductor L is discharged and delivers its stored energy to C_1 and R_1 , so inductor current is decreased. In this state, C_1 is charged and C_2 is discharged and delivers its stored energy to load resistance R_2 . The energy storage elements L , C_1 , and C_2 equations in this mode are as follows:

$$\begin{cases} L \frac{dI_L}{dt} = (V_{in1} - V_{O1}) \\ C_1 \frac{dV_{O1}}{dt} = I_L - \frac{V_{O1}}{R_1} \\ C_2 \frac{dV_{O2}}{dt} = -\frac{V_{O2}}{R_2} \end{cases} \quad (3)$$

4) *Switching State 4* ($D_4 T < t < T$): In this mode, all of three switches are OFF. So, diode D_2 is forward biased. In this state, inductor L is discharged and delivers its stored energy to capacitors C_1 , C_2 , and load resistances R_1 and R_2 . Also, in this mode, capacitors C_1 and C_2 are charged. Equivalent circuit of proposed converter in this state is shown in Fig. 4(d). The inductor and capacitors equations in this mode are as follows:

$$\begin{cases} L \frac{dI_L}{dt} = V_{in1} - (V_{O1} + V_{O2}) \\ C_1 \frac{dV_{O1}}{dt} = I_L - \frac{V_{O1}}{R_1} \\ C_2 \frac{dV_{O2}}{dt} = I_L - \frac{V_{O2}}{R_2} \end{cases} \quad (4)$$

2.2 Battery charging mode

In this mode, V_{in1} supplies load as well as supplies V_{in2} battery also. This condition occurs when load requirement is low and battery has to be charge. When battery operates at charging mode, in such condition, S_3 is not active and switches S_1 , S_2 , S_4 , are active. Here switch S_2 is on to control battery current to desired value by controlling inductor current. Switch S_1 regulate the total output voltage $V_T = V_{O1} + V_{O2}$ and output voltage V_{O1} is regulate by switch S_4 . In Fig. 5 inductor voltage, Inductor current and gate signal of the switch waveforms are presented. In one switching period there are four different operation modes.

1) *Switching State 1* ($0 < t < D_1 T$): In this mode S_1 is active, so S_4 and S_2 reverse biased. D_2 also reversely biased. So, inductor L charges by V_{in2} and inductor current increases. In this mode, capacitors C_1 and C_2 supplies energy to the load resistances R_1 and R_2 . Equivalent circuit of this switching state shown in Fig. 6(a). The equations of inductor and capacitors are as follows:

$$\begin{cases} L \frac{dI_L}{dt} = V_{in1} \\ C_1 \frac{dV_{O1}}{dt} = -\frac{V_{O1}}{R_1} \\ C_2 \frac{dV_{O2}}{dt} = -\frac{V_{O2}}{R_2} \end{cases} \quad (5)$$

2) *Switching State 2* ($D_1 T < t < D_2 T$): In this mode, switch S_1 is OFF and switch S_2 is active. $V_{in1} < V_{in2}$, so inductor current decreases and delivered energy to the battery (V_{in2}). In this mode, capacitors C_1 and C_2 get discharged and supplies energy to the load resistances R_1 and R_2 . Equivalent circuit of this switching state shown in Fig. 6(b) and equations are

$$\begin{cases} L \frac{dI_L}{dt} = (V_{in1} - V_{in2}) \\ C_1 \frac{dV_{O1}}{dt} = -\frac{V_{O1}}{R_1} \\ C_2 \frac{dV_{O2}}{dt} = -\frac{V_{O2}}{R_2} \end{cases} \quad (6)$$

3) *Switching State 3* ($D_2 T < t < D_4 T$): In this mode, S_2 is turned OFF and switch S_4 is turned ON switch and S_1 is still OFF. Also, diode D_2 is reversely biased. In Fig. 6(c), equivalent circuit of proposed converter in this state is shown. In this state, inductor L is discharged and delivers its stored energy to C_1 and R_1 , and capacitors C_1 is charged and capacitor C_2 is discharged and delivers its stored energy to load resistance R_2 . Equations of this state are follows:

$$\begin{cases} L \frac{dI_L}{dt} = (V_{in1} - V_{O1}) \\ C_1 \frac{dV_{O1}}{dt} = I_L - \frac{V_{O1}}{R_1} \\ C_2 \frac{dV_{O2}}{dt} = -\frac{V_{O2}}{R_2} \end{cases} \quad (7)$$

4) *Switching State 4* ($D_4 T < t < T$): In this mode, all switches are OFF. Inductor L is discharged through the diode D_2 which is forward biased and delivers its stored energy to resistors R_1, R_2 and charges capacitors C_1 and C_2 . Fig. 6(d) shown the equivalent circuit and circuit equations are as follows:

$$\begin{cases} L \frac{di_L}{dt} = V_{in1} - (V_{O1} + V_{O2}) \\ C_1 \frac{dV_{O1}}{dt} = I_L - \frac{V_{O1}}{R_1} \\ C_2 \frac{dV_{O2}}{dt} = I_L - \frac{V_{O2}}{R_2} \end{cases} \quad (8)$$

3 MODELING OF THE CONVERTER

Dynamic model is needed for design the closed loop controller for the converter. By proper switching dutycycles, output voltages and battery current are adjustable. There are different dynamic models for each operation modes of converter. Consequently, for both operation modes, different controller needs to be designed separately. To realize closed-loop control Small-signal model is used. Based on small-signal modeling method, the state variables, duty ratios, and input voltages contain two components, dc values (X, D, V) and perturbations ($\hat{x}, \hat{d}, \hat{v}$). It is assumed that the perturbations are small and do not vary significantly during one switching period.

3.1 Battery discharging mode

In this mode the system can be represented in a matrix form using a state-space model such that $i_L(t), v_{O1}(t),$ and $v_{O2}(t)$ are state variables.

$$\begin{cases} \frac{dx}{dt} = AX + BU \\ Y = CX + BU \end{cases} \quad (9)$$

$$X = \begin{bmatrix} \hat{i}_L(t) \\ \hat{v}_{O1}(t) \\ \hat{v}_{O2}(t) \end{bmatrix} \quad Y = \begin{bmatrix} \hat{v}_{O1}(t) \\ \hat{v}_T(t) \\ \hat{i}_b(t) \end{bmatrix} \quad U = \begin{bmatrix} \hat{d}_4(t) \\ \hat{d}_3(t) \\ \hat{d}_1(t) \end{bmatrix} \quad (10)$$

U is a matrix containing the control inputs $d_1(t), d_3(t)$ and $d_4(t)$, and Y is a matrix containing the system outputs $v_{O1}(t), v_T(t),$ and $i_b(t)$. Filling in the A, B, C, and D matrices using (1)-(4) and state equations (9), and using the equation for unknown inductor current gives the unknown parameters D_1, D_3, D_4 .

$$I_L = \frac{I_b}{D_3} \quad (11)$$

The values of switches duty cycles are obtained by steady-state equations which expressed in following equation:

$$\begin{bmatrix} V_{O1} & V_{in2} - V_{in1} & V_{O2} \\ R_1 I_b & V_{O1} & 0 \\ 0 & V_{O2} & R_2 I_b \end{bmatrix} \begin{bmatrix} D_1 \\ D_3 \\ D_4 \end{bmatrix} = \begin{bmatrix} V_{O1} + V_{O2} - V_{in1} \\ R_1 I_b \\ R_2 I_b \end{bmatrix} \quad (12)$$

The transfer function matrix of the converter is obtained from the small signal model as follows:

$$G = (SI - A)^{-1}B + D \quad (13)$$

Where

$$y = Gu \quad (14)$$

$$\begin{bmatrix} y_1 \\ y_2 \\ y_3 \end{bmatrix} = \begin{bmatrix} g_{11} & g_{12} & g_{13} \\ g_{21} & g_{22} & g_{23} \\ g_{31} & g_{32} & g_{33} \end{bmatrix} \begin{bmatrix} u_1 \\ u_2 \\ u_3 \end{bmatrix} \quad (15)$$

Where y and u are the system output and input vectors, and component g_{ij} represents the transfer function between y_i and u_j . So, there are three transfer functions as follows:

$$\begin{cases} g_{11} = \frac{\hat{v}_{O1}(s)}{\hat{d}_4(s)} \\ g_{22} = \frac{\hat{v}_T(s)}{\hat{d}_3(s)} \\ g_{33} = \frac{\hat{i}_b(s)}{\hat{d}_1(s)} \end{cases} \quad (16)$$

3.1 Battery charging mode

Like battery discharging mode, first small signal model should be obtained. In this mode the system can be represented in a matrix form using state-space model such that $i_L(t), v_{O1}(t),$ and $v_{O2}(t)$ are state variables. State variables, input, and output matrices are illustrated as follows:

$$X = \begin{bmatrix} \hat{i}_L(t) \\ \hat{v}_{O1}(t) \\ \hat{v}_{O2}(t) \end{bmatrix} \quad Y = \begin{bmatrix} \hat{v}_{O1}(t) \\ \hat{v}_T(t) \\ \hat{i}_b(t) \end{bmatrix} \quad U = \begin{bmatrix} \hat{d}_4(t) \\ \hat{d}_1(t) \\ \hat{d}_2(t) \end{bmatrix} \quad (17)$$

U is a matrix containing the control inputs $d_1(t), d_2(t)$ and $d_4(t)$, and Y is a matrix containing the system outputs $v_{O1}(t), v_T(t),$ and $i_b(t)$. Filling in the A, B, C, and D matrices using (5)-(8) and state equations (9), and using the equation for unknown inductor current gives the unknown parameters D_1, D_2, D_4 .

$$I_L = \frac{I_b}{D_2 - D_1} \quad (18)$$

The values of switches duty cycles are obtained by steady-state equations which expressed in following equation:

$$\begin{bmatrix} V_{in2} & V_{O1} - V_{in1} & V_{O2} \\ -V_{O1} & V_{O1} + R_1 I_b & 0 \\ -V_{O2} & V_{O2} & R_2 I_b \end{bmatrix} \begin{bmatrix} D_1 \\ D_2 \\ D_4 \end{bmatrix} = \begin{bmatrix} V_{O1} + V_{O2} - V_{in1} \\ R_1 I_b \\ R_2 I_b \end{bmatrix} \quad (19)$$

The transfer function matrix of the converter is obtained from the small signal model as follows:

$$G = (SI - A)^{-1}B + D \quad (20)$$

Where

$$y=Gu \tag{21}$$

$$\begin{cases} g_{11} = \frac{v_{O1}(s)}{d_4(s)} \\ g_{22} = \frac{v_T(s)}{d_1(s)} \\ g_{33} = \frac{i_b(s)}{d_2(s)} \end{cases} \tag{22}$$

4 CONTROLLER DESIGN

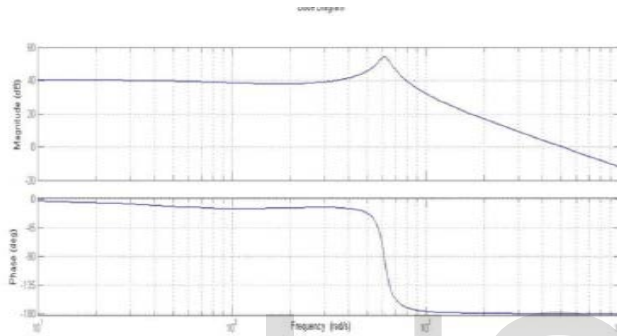


Fig. 7 Simulated Bode plot of $g_{11}(s)$ before applying controller.

er.

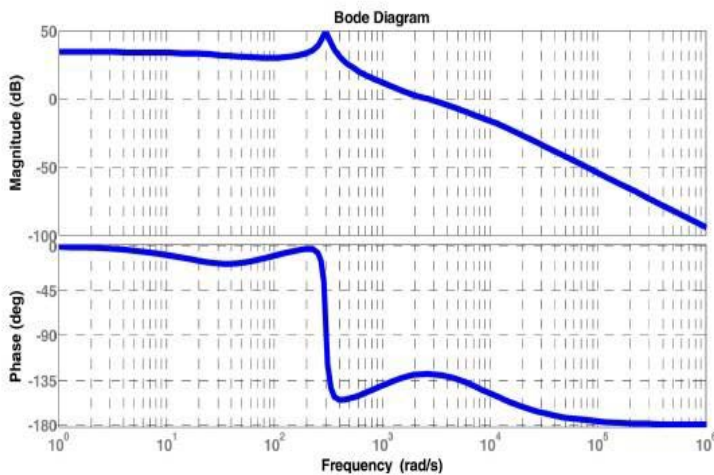


Fig. 8 Simulated Bode plot of $g_{11}(s)$ after applying controller.

For each mode we have three transfer functions. For each transfer function, frequency-domain bode plot analysis need to be obtained by computer software to design the system com-

pensators. System compensators should provide desired steady-state error and sufficient phase margin, high stability, and high bandwidth. Utilizing A, B, C, and D matrices and transfer function matrix G, transfer function of each switching state can be obtained. By using MATLAB software bode plot analysis obtained. Open loop bode diagram of the transfer function g_{11} shown in Fig. 7. Phase margin of the plot is 91° which is not sufficient. To increase the phase margin and system stability a lead compensator introduced.

$$K(S) = \frac{S+Z}{S+P} \tag{23}$$

After compensation the stability of the system also improves as shown in Fig. 8. From bode plot understood that in switching state 1,2 and 3 lead compensator, lead-lag compensator and lag compensator is required. Like battery discharging mode in, battery charging mode also bode plot analyzed. From bode plot understood that in switching state 1,2 and 3 lead-lag compensator, lead compensator and lag compensator is required.

5 SIMULATION RESULTS

TABLE 1

Simulation and prototype parameters

Simulation and prototype parameters	Symbol
1.3 mH	L
1000 μ F	C_1
1000 μ F	C_2
24 V	V_{in1}
34 V	V_{in2}
10 kHz	f_s

Simulations have been done in MATLAB software. The simulation parameters of the converter are listed in Table I. Input voltage sources are considered $V_{in1} = 24V$, $V_{in2} = 36V$. In simulations, battery model is used as input source 2. Inductor

$L=1.3\text{mH}$ and the $R_1 = 27\Omega$ and $R_2 = 27\Omega$ are the load resistances, which can represent the equivalent power feeding a multilevel inverter.

The input voltage is given by $V_{in1}=24\text{ V}$ shown in figure 9. The gate signals are given from PWM block. In figure 10 inductor current is shown. The battery current shown in figure 11 with average value of 1.1 V. The output voltages shown in figure 12. The total voltage V_T is regulated to 48 V and V_{O1} is regulated to 24V.

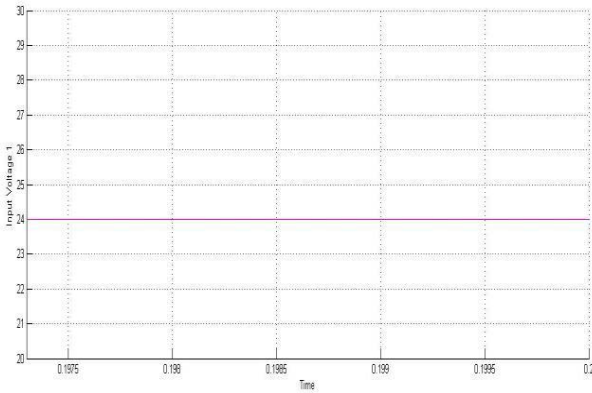


Fig.9 input voltage V_{in1} .

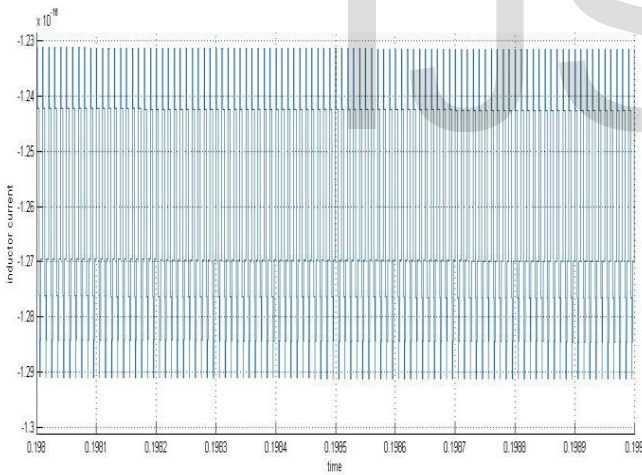


Figure.10 Inductor current I_L .

Fig.11 Battery current I_b

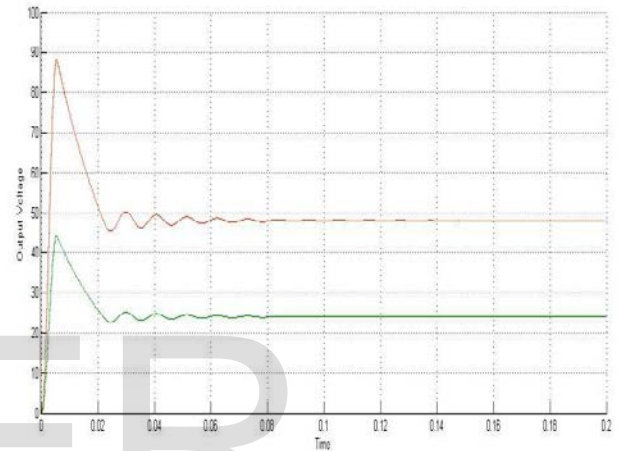


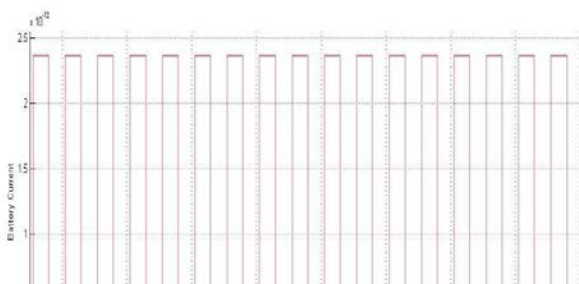
Fig.12 Output voltage V_T and V_{O1}

6 CONCLUSION

A new multiinput multioutput dc–dc boost converter is proposed in this paper. The proposed converter can be used for transferring energy between different energy resources. In this paper, FC and battery is used as energy sources. The converter has two main operating modes in which battery discharging mode both FC and battery deliver power to load and in charging mode, FC deliver power to load and battery. It has several outputs with different voltage levels which makes it suitable for interfacing to multilevel inverter. Using multilevel inverters in electric vehicles, leads to torque ripple reduction of induction motors. This converter is also suitable for electric vehicle electric which uses two different dc voltage levels, one for ventilation system and cabin lightening and other for supplying dc motor.

REFERENCES

- [1] port bidirectional converter for hybrid fuel cell systems,” in P. Thounthong, V. Chunkag, P. Sethakul, B. Davat, and M. Hinaje “Comparative study of fuel-cell vehicle hybridization with bat-



- tery or supercapacitor storage device," *IEEE Trans. Veh. Technol.*, vol. 58, no. 8, pp.3892–3905, Oct. 2009.
- [2] M. Michon, J. L. Duarte, M. A. M. Hendrix, and M. G. Simes, "A three phase Proc. 35th Annu. IEEE Power Electron. Spec. Conf., Aachen, Germany, 2004, pp.4736–4741.
- [3] H. Tao, A. Kotsopoulos, J. L. Duarte, and M. A. M. Hendrix, "Family of multiport bidirectional DC–DC converters," *Inst. Electr. Eng. Proc. Elect. Power Appl.*, vol. 153, no. 3, pp. 451–458, May 2006
- [4] H. Tao, J. Duarte, and M. Hendrix, "Three-port triple-half-bridge bidirectional converter with zero-voltage switching," *IEEE Trans. Power Electron.*, vol. 23, no. 2, pp. 782–792, Mar. 2008.
- [5] E. H. Krishnaswami and N. Mohan, "Three-port series-resonant DC–DC converter to interface renewable energy sources with bidirectional load and energy storage ports," *IEEE Trans. Power Electron.*, vol. 24, no. 10, pp. 2289–2297, Oct. 2009.
- [6] H. Wu, K. S. Ding, and Y. Xing, "Topology derivation of nonisolated three-port DC–DC converters from DIC and DOC," *IEEE Trans. Power Electron.*, vol. 28, no. 7, pp. 3297–3307, Jul. 2013.
- [7] V. A. K. Prabhala, D. Somayajula and M. Ferdowsi, "Power sharing in a double-input buck converter using dead-time control," in *Proc. Energy Convers. Congr. Expo.*, 2009.
- [8] Z. Li, O. Onar, and A. Khaligh, "Design and control of a multiple input DC/DC Converter for battery/ultra capacitor based electric vehicle power system" in *Proc. IEEE Twenty-Fourth Annu. Appl. Power Electron. Conf. Expo.*, 2009.
- [9] K. Gummi and M. Ferdowsi, "Double-input DC-DC power electronic converters for electric-drive vehicles – topology exploration and synthesis using a single-pole triple-throw switch," *IEEE Trans. Ind. Electron.*, vol. 57, no. 2, pp. 617–621, Feb. 2010.
- [10] T. Bhattacharya, V. S. Giri, K. Mathew, and L. Umanand, "Multi phase bidirectional flyback converter topology for hybrid electric vehicles," *IEEE Trans. Ind. Electron.*, vol. 56, no. 1, pp. 78–83, Jan. 2009.
- [11] R. Ahmadi and M. Ferdowsi, "Double-input converter on half-bridge cells: derivation, small-signal modeling, and power sharing analysis" *IEEE Trans. Circuit Syst.*, vol. 59, no. 4, pp. 875–889, Apr. 2012
- [12] O. C. Onar and A. Khaligh, "A novel integrated magnetic structure based DC/DC converter for hybrid battery/ultracapacitor energy storage systems," *IEEE Trans. Smart Grid*, vol. 3, no. 1, pp. 782–792, Mar. 2008.
- [13] S. Danyali, S.H. Hosseini, and G. B. Gharehpetian, "New extendable single stage multi-input DC–DC/AC boost converter," *IEEE Trans. Power Electron.*, vol. 29, no. 2, pp. 775–788, Feb. 2014.
- [14] H. Behjati and A. Davoudi, "A MIMO topology with series outputs: An interface between diversified energy sources and diode-clamped multilevel inverter," in *Proc. Appl. Power Electron. Conf. Expo.*, 2012.
- [15] H. Behjati and A. Davoudi, "A multi-port DC–DC converter with independent outputs for vehicular applications," in *Proc. Vehicle Power Propulsion Conf.*, 2011.
- [16] Y. Ch. Liu and Y. M. Chen, "A systematic approach to synthesizing multiinput DC–DC converters," *IEEE Trans. Power Electron.*, vol. 24, no. 1, pp. 116–127, Jan. 2009.
- [17] A. Kwasinski, "Identification of feasible topologies for multiple-input DC–DC converters," *IEEE Trans. Power Electron.*, vol. 24, no. pp. 856–861, Mar. 2010.
- [18] A. Khaligh, J. Cao, and Y. J. Lee, "A multiple-input DC–DC converter topology," *IEEE Trans. Power Electron.*, vol. 24, no. 3, pp. 862–868, Mar. 2009.
- [19] Zh. Qian, O. A. Rahman, and I. Batarseh, "An integrated four-port DC/DC converter for renewable energy applications," *IEEE Trans. Power Electron.*, vol. 25, no. 7, pp. 1877–1887, Jul. 2010.
- [20] M. Sarhangzadeh, S. H. Hosseini, M. B. B. Sharifian, and G. B. Gharehpetian, "Multi-input direct DC-AC converter with high frequency link for clean power generation systems," *IEEE Trans. Power Electron.*, vol. 26, no. 6, pp. 625–631, Jun. 2011.
- [21] H. Tao, J. L. Duarte, and M. A. M. Hendrix, "Line-interactive UPS using a fuel cell as the primary source," *IEEE Trans. Ind. Electron.*, vol. 51, no. 3, pp. 3012–3021, Aug. 2008.
- [22] Y. Zhou and W. Huang, "Single-stage boost inverter with coupled inductor," *IEEE Trans. Power Electron.*, vol. 27, no. 4, pp. 1885–1893, Apr. 2012.
- [23] L. Solero, A. Lidozzi, and J. A. Pomilio, "Design of multiple-input power converter for hybrid vehicles," *IEEE Trans. Power Electron.*, vol. 20, no. 5, pp. 1007–1016, Sep. 2005.
- [24] K. Ogata, *Modern Control Engineering*. Englewood Cliffs, NJ, USA: Prentice-Hall, 2002.
- [25] X. Zhang and C. Mi, *Vehicle Power Management*, New York, NY, USA: Springer, 2011.
- [26] A. Emadi; K. Rajashekar; S.S. Williamson; S.M. Lukic, "Topological overview of hybrid electric and fuel cell vehicular power system architectures and configurations," *Vehicular Technology, IEEE Transactions on*, vol. 54, no. 3, pp. 763–770, May 2005.
- [27] A. Emadi; S.S. Williamson; A. Khaligh, "Power electronics intensive solutions for advanced electric, hybrid electric, and fuel cell vehicular power systems," *Power Electronics, IEEE Transactions on*, vol. 21, no. 3, pp. 567–577, May 2006.
- [28] A. Emadi; S.S. Williamson; A. Khaligh, "Power electronics intensive solutions for advanced electric, hybrid electric, and fuel cell vehicular power systems," *Power Electronics, IEEE Transactions on*, vol. 21, no. 3, pp. 567–577, May 2006.
- [29] A. Khaligh; Li. Zhihao, "Battery, Ultracapacitor, Fuel Cell, and Hybrid Energy Storage Systems for Electric, Hybrid Electric, Fuel Cell, and Plug-In Hybrid Electric Vehicles: State of the Art," *Vehicular Technology, IEEE Transactions on*, vol. 59, no. 6, pp. 2806–2814, July 2010.
- [30] D. Yu, Z. Xiaohu, B. Sanzhong, S. Lukic, A. Huang, "Review of non-isolated bi-directional DC-DC converters for plug-in hybrid electric vehicle charge station application at municipal parking decks," *IEEE Appl. Power Electron. Conf. and Expo., (APEC), 2010*, pp. 1145–1151, Feb. 2010